Published in final edited form as:
J Phys Chem B. 2011 July 7; 115(26): 8371–8380. doi:10.1021/jp201235m.

Bioelectronic Delivery of Electrons to Cytochrome P450 Enzymes

Sadagopan Krishnan[†,£], **John B. Schenkman**[§], and **James F. Rusling**[†,§,*]
Department of Chemistry, University of Connecticut, Storrs, Connecticut 06269, Department of Cell Biology, University of Connecticut Health Center, Farmington, Connecticut 06032

[†] Dept. of Chemistry, University of Connecticut.

[§] Dept. of Cell Biology, University of Connecticut Health Center.

Abstract

Cytochrome P450s (cyt P450s) are the major oxidative enzymes in human oxidative metabolism of drugs and xenobiotic chemicals. In nature, the iron heme cyt P450s utilize oxygen and electrons delivered from NADPH by a reductase enzyme to oxidize substrates stereo- and regioselectively. Significant research has been directed toward achieving these events electrochemically. This feature article discusses the direct electrochemistry of cyt P450s in thin films, and the utilization of such films for electrochemically-driven biocatalysis. Maintaining and confirming structural integrity and catalytic activity of cyt P450s in films is an essential feature of these efforts. We highlight here our efforts to elucidate the influence of iron heme spin state and secondary structure of human cyt P450s on voltammetric and biocatalytic properties, using methodologies to quantitatively describe the dynamics of these processes in thin films. We also describe the first cyt P450/reductase films that accurately mimic the natural biocatalytic pathway, and show how they can be used with voltammetry to elucidate key mechanistic features. Such bioelectronic cyt P450 systems have high value for future drug development, toxicity screening, fundamental investigations, and chemical synthesis systems.

I. Introduction

Cytochrome P450s (cyt P450s) are iron heme monooxygenase enzymes that are catalysts for oxidative metabolism of ~75% of drugs and foreign lipophilic compounds.[1,2] Oxidative metabolites generated by cyt P450s may be easily cleared from the body, or may elicit toxic effects by reactions with biomolecules such as DNA and proteins.[3] Attractive chemical features of cyt P450s arise from their unique catalytic properties, wide substrate utilization, stereoselectivity, regiospecificity, and broad and unique catalytic reactions. Despite intense research efforts over nearly a half-century, some details of the catalytic pathways of cyt P450s are still not understood completely.[2] However, significant progress has been made in understanding the redox chemistry of cyt P450s and their metabolic pathways, and in solving the crystal structures of cyt P450 isoforms. Crystal structures of human cyt P450s 1A2,[4] and 2E1,[5] and bacterial cyt $P450_{cam}$[6] are shown in Figure 1. The catalytic site is the iron heme cofactor bound to the enzyme by an Fe-S linkage.

The catalytic cycle of cyt P450s (Scheme 1) features delivery of electrons from cyt P450 NADPH-reductase (CPR) to cyt P450s, probably within a transient CPR-cyt P450 complex. Specifically substrate first binds to the cyt P450 in a pocket above the Fe^{III} heme, followed

[*]Corresponding author james.rusling@uconn.edu.
[£]Present address: Inorganic Chemistry Laboratory, Oxford University, Oxford, UK.

by electron donation from NADPH via CPR to form cyt P450-Fe^{II} heme.[2] Dioxygen then binds to the cyt P450-Fe^{II} heme, followed by a second electron transfer from CPR. Protonation results in the cyt P450-Fe^{III}-hydroperoxo complex **6**. In some cases, cytochrome b_5 can facilitate the second electron transfer.[8,9] The cyt P450-Fe^{III}-hydroperoxo complex can also be generated using hydrogen peroxide or an organic peroxide, which bypasses the need for NADPH, cyt P450-reductase, and molecular oxygen.[10] Further protonation of **6** followed by elimination of water yields $^{+\bullet}$(P450-Fe^{IV}=O) [**7**, Scheme 1]. This ferryloxy radical cation form of cyt P450s is presumed to be the active oxidant that transfers oxygen to the bound substrate (RH) to form product (ROH). Bacterial cyt $P450_{cam}$, on the other hand, requires iron-sulfur protein (putidaredoxin) as a redox partner to deliver electrons from NADPH.[2] Mammalian P450scc, sterol 27-hydroxylase and P45011β are mitochondrial enzymes that make use of a non-heme iron sulfur redox protein, and not CPR.[2]

Carbon monoxide binds to the reduced form of cyt P450s yielding cyt P450-Fe^{II}-CO heme that can be monitored spectroscopically from the characteristic difference absorbance band at 450 nm, from which cyt P450s get their name.[1,2] Full details on the biochemistry of cyt P450s and mechanisms of catalytic reactions can be found in references 1 and 2, and recent reviews.[11,12] There are ~57 known cyt P450 isoforms in humans[13] with many of them present in the liver where they are involved in xenobiotic metabolism.[14] Due to ease of isolation and purification, bacterial cyt $P450_{cam}$ or CYP101 has been more extensively studied compared to mammalian cyt P450s.

It has long been a dream to activate cyt P450s electronically, thereby bypassing electron donation from NADPH.[15] Hill et al. reported the first direct bacterial cyt $P450_{cam}$ electrochemistry in 1996 using highly purified enzyme in low temperature solution.[16] Shortly thereafter, we described the first direct voltammetry of cyt $P450_{cam}$ in thin films of insoluble surfactants[18] and polyions.[19] Since that time, there has been considerable research involving cyt P450 thin film voltammetry. Much of this work is summarized in reviews, including articles by Scheller et al. covering direct electrochemistry and biosensors,[20] Fleming et al.[21] addressing large-amplitude Fourier transform ac voltammetry, and Gilardi et al.[22] discussing electrochemistry of cyt P450s, microsomes, and fusion proteins with emphasis on genetic engineering.

Fusion proteins feature the advantage that proteins like flavodoxin or the reductase domain of CPR linked to a cyt P450 can accept electrons from an electrode and inject them into the enzyme to drive catalytic processes.[22] On the other hand, electrochemical biocatalysis utilizing *direct* electron transfer to cyt P450s in films in aerobic solution features enzyme-catalyzed reduction of oxygen to hydrogen peroxide, which in turn reacts with cyt P450Fe^{III} to form the active ferryloxy species that oxidizes substrates.[19-26] Neither approach fully mimics the natural catalytic pathway, which is desirable to retain all catalytic properties and features of the enzyme pathways. Thus, a specific unmet research challenge has been to deliver electrons from electrode to CPR to cyt P450s to drive the natural catalytic cycle electrochemically.[27-29] Such “bioelectronic” cyt P450 activation avoids expensive NADPH, enables probing the catalytic pathway with voltammetric kinetic analyses, and facilitates electronically-driven bioreactor and biosensor applications. A purpose of this feature article is to describe our successful endeavors in using electrons from an electronic source for donation to CPR, then to cyt P450s, to directly mimic the natural catalytic pathway on an electrode. In the following sections, we first summarize research on thin film cyt P450 voltammetry and biocatalysis in a bit more detail, and then discuss voltammetric kinetic studies that have provided insights into electron transfer dynamics of human cyt P450s. Finally, we describe a novel film system combining CPR microsomes with excess human cyt P450s designed to closely mimic the natural cyt P450 catalytic cycle.

II. Overview of thin film voltammetry and biocatalysis with cyt P450s

The importance of protein purity and surface chemistry of electrodes in achieving direct voltammetry of proteins in solution began to be realized in the 1970s.[30-32] An early attempt at voltammetry of cyt P450s used microsomal preparations in solution, but electron transfer to cyt P450 was not achieved.[33] Several proteins and small molecules that deliver electrons to the enzyme have been used to mediate electron transfer and catalytic reactions of cyt P450s.[34-36]

Protein film voltammetry (PFV) was a huge breakthrough in direct protein electrochemistry and electrochemical biocatalysis.[37-39]$_{In}$ this method, a thin film of protein often utilizing other materials such as polyions, self-assembled monolayers (SAM), or lipids is deposited on an electrode in a stable film in which the protein retains native conformation.[25] PFV has significant advantages over solution voltammetry: (a) it negates the need for mediators; (b) it eliminates diffusion of large protein molecules and electrode fouling by denatured protein; and (c) the simple procedure requires only tiny amounts of protein.

Both covalent and non-covalent approaches to immobilize cyt P450s on electrodes have been reported (Scheme 2). Films of cyt P450s and insoluble surfactants, lipids, DNA, or polyions, as well as electrostatically adsorbed films prepared layer-by-layer (LbL) of cyt P450s and oppositely charged polyions have provided direct film voltammetry.[20-22,25,26] Davis and Hill used scanning probe microscopy to characterize cytP450$_{cam}$ monolayers on Au suitable for direct voltammetry.[40] Covalent immobilization includes the use of self-assembled monolayers,[41] and electrodes modified with maleimide group to orient cyt P450s via cysteine residues.[42-45] Scheller reviewed direct electron transfer studies and electrocatalysis of cyt P450s up to 2004.[20]

An important objective is to achieve efficient biocatalysis for synthetic and biosensor applications.[25,26,46] Cyt P450 catalysis is a complex multistep process in which initial reduction of enzyme and reaction with oxygen leads to the active reductant (Scheme 1). A number of experimental parameters including oxygen content need to be optimized.[28] Fast electron transfer may not directly correlate with catalytic efficiency. For example, Gilardi et al. reported larger catalytic efficiency for cyt P450 3A4-CPR fusion protein films on Au electrodes compared to glassy carbon, although the Au system showed smaller direct electron transfer rates.[47]

Figure 2 shows examples of background subtracted CVs with increasing scan rates for pure human cyt P450 2E1 and bacterial P450$_{cam}$ LbL films assembled with polyions on pyrolytic graphite (PG) electrodes.[48] This method is particularly versatile, and provides stable films from stepwise deposition of biomolecules and/or synthetic polyions by reversing charge at each deposition step.[17,49] Weakly adsorbed molecules are washed away between each deposition step, thus selecting out only the strongest interactions. The formal potential for cyt P450s-polyion LbL films on PG electrodes is about -350 mV vs SCE, pH 7.0, 25 °C.[48]

It is important to maintain and confirm native enzyme structures in the films. Structural integrity of cyt P450s is easily ascertained by chemically reducing the enzyme and adding carbon monoxide. The appearance of a cyt P450Fe^{II}-CO difference absorbance band near 450 nm is characteristic of the native enzyme (Figure 3A-D), while a band at 420 nm indicates denatured enzyme.[2] Also, the spectrum of cyt P450-Fe^{III} (Figure 3 E, F) should closely resemble the spectrum in solution. It is important to realize, however, that spectra of proteins in solutions containing the materials to be used for films provide little information about protein structure in the films themselves, since refolding toward native states as well as unfolding can occur during film formation or upon variations in electrolyte solutions.[50-52]

Absorbance spectra of cyt P450s in films on aminosilane functionalized silica slides confirming native cyt P450 in these films are shown in Figure 3.[48,53,76]

The lipid dimyristoyl phosphatidylcholine and insoluble surfactant didodecyldimethylammonium bromide (DDAB) comprised the first films in which reversible voltammetry of cyt $P450_{cam}$ was observed.[18] There has been some concern about instability and loss of catalytic activity of heme proteins including cyt P450s in DDAB films, although the original paper presented the 450 nm cyt P450-Fe^{II}-CO spectral band confirming native structure. It has not always been realized that solution pH and the presence of Br^- in film preparation and voltammetry buffers are critical to retain structural integrity of heme proteins in DDAB films.[54] The presence of Br^- stabilizes DDAB in an insoluble bilayer structure[55] that also favors retention of near native structures of heme proteins. With other electrolyte anions in the solution, most notably acetate, DDAB forms soluble micellar structures[55] that may denature proteins and degrade film stability. Heme proteins in DDAB films made with neutral pH NaBr-containing buffers and used in pH 5-7 buffers containing 50 mM NaBr retained near-native conformations as characterized by absorbance and circular dichroism spectra.[54] These conclusions were confirmed recently by Lee and Bond using higher order harmonics of large-amplitude Fourier transformed AC voltammetry.[56] Also, cyt $P450_{cam}$ in DDAB films was active for epoxidation of styrene to styrene oxide from electrolysis using $P450_{cam}$-DDAB films on carbon cloth electrodes.[23] Thus, structural integrity and catalytic activity of cyt P450s in surfactant films require careful control of conditions such as pH and Br^- content used to make and analyze the films. A caveat is to beware of Br^- in electrolytes with gold electrodes, since surface Br^- complexes can produce spurious peaks.[57]

No catalytic activity of cyt P450 BM3 in DDAB films was found using voltammetry. Detailed spectral and electrochemical analyses suggested the existence of a P420-like state of this enzyme in the DDAB films.[58] However, the stabilizing effect of NaBr on cyt P450 BM3-DDAB films was not evaluated. Ohno et al. concluded from Raman spectra that thermophilic cyt P450st in DDAB films on plastic-formed carbon (PFC) electrodes retained near-native conformation when NaBr was included in the buffer.[59] However, they did not observe voltammetric peaks of P450st in these films. On the other hand, thermophilic cyt P450 CYP119 was earlier shown to exhibit reversible voltammetry in DDAB films.[60] Electrocatalytic reduction of nitrite, nitric oxide, carbon tetrachloride, and nitrous oxide was catalyzed using CYP119/DDAB films and corresponding products were confirmed.[61,62]

Shumyantseva et al. obtained well defined CVs and good catalytic activity for cyt P450 2B4 in gold nanoparticle-DDAB films (DDAB/Au/P450 2B4) on screen-printed graphite electrodes. [63] They obtained comparable electrochemically-driven turnover rates for N-demethylation of benzphetamine using DDAB/Au/P450 2B4 films and a microsomal system and NADPH. Gilardi et al. covalently immobilized cyt P450 2E1 via a cysteine residue with maleimide surface groups on gold electrodes (Au/CYSAM/MALIM/P450 2E1).[43] These electrodes were catalytically active and exhibited an increase in catalytic current with increasing p-nitrophenol concentration. Electrolysis product p-nitrocatechol was quantified.[43]

Cyt P450 1A2/polyion LbL films were used to convert styrene to styrene oxide.[64] This reaction is driven in aerobic solutions by electrochemically formed hydrogen peroxide from the reduction of P450Fe^{II}-O_2 on the electrode and its reaction with P450Fe^{III} forming the active ferryloxy-cyt P450 that epoxidized styrene (see Scheme 4A). Comparable enzyme turnover rates were found for electrolysis and activation by adding hydrogen peroxide. The turnover rate for cyt P450 1A2 in solution utilizing NADPH and CPR to metabolize styrene was nearly half of that of electrolysis suggesting good catalytic efficiency of the electrode

film system. Our study showed that interlayer-mixing in LbL films and electron hopping facilitate charge transport over film thicknesses of 40-320 nm for LbL films of heme proteins including cyt P450cam. Films of <50 nm thick with 2 or 3 layers of enzyme gave larger catalytic turnover rates as they were not subject to mass transport limitations as were thicker films.[24] Taken together, the above studies suggest that catalytic efficiency achieved by electrode driven cyt P450 catalysis using direct electron transfer can be comparable to solution reactions using reagents such as peroxides, or NADPH and reductases.

III. Electron transfer model for PFV of cyt P450s

Laviron's theory describes the voltammetry of surface confined molecules[65] and is widely used to estimate electron transfer rate constants from increases in reduction-oxidation peak separations with increasing CV scan rate. However, the frequent observation of scan rate-independent peak separation at low scan rates in CVs of redox molecules is not consistent with Laviron's model. Feldberg and Rubinstein described an N-shaped free energy relationship to account for non-kinetic hysteresis observed in CVs including the scan rate independent peak separation at low scan rates.[66] This was later attributed to conformational differences in oxidized and reduced forms of the protein, explained using a square scheme by Bowden et al.[67] This interpretation was consistent with the observed conformational differences in oxidized and reduced forms of many proteins.[25,26,68] Hirst and Armstrong suggested subtracting the constant, non-kinetic, low scan rate peak separation from values at higher scan rates, then calculating heterogeneous electron transfer (hET) rate constants using Laviron theory.[69] This eliminates errors from non-kinetic hysteresis in CVs, and often provides hET rate constants of proteins that give excellent fits to the Laviron model. In such cases, rate constant values are independent of scan rate showing that they fit the model, but this is not the case if large non-kinetic corrections are ignored.

We recently related electrochemical electron transfer kinetics of cyt P450s in ultrathin polyion films to enzyme electronic and secondary structure for the first time.[48] Near native enzyme structures in the films were confirmed by spectra representing known high and low spin ferric heme bands of cyt P450s and by the 450 nm bands of cyt P450Fe^{II}-CO complexes (Figure 3). CO binding to reduced cyt P450s was confirmed electrochemically by 38-50 mV positive midpoint potential shifts in CVs.[48]

Representative CVs are shown in Figure 2. Good agreement between the corrected experimental peak separations (symbols) and the Laviron surface voltammetry model (lines) allowed the estimation of average hET rate constants, k_s (Figure 4).[48] Plots of the variation of individual reduction and oxidation peak potentials with scan rate, called *trumpet plots*, provide an additional tool for mechanistic analysis.[37] Trumpet plots for the three cyt P450s did not follow Laviron theory (Figure 5), which predicts that they should be symmetrical. Asymmetry is most prominent for cyt P450 2E1 (Figure 5B), in which the reduction peak potential varies much more than the oxidation peak potential as scan rate increases.

Scheme 3 includes conformational changes coupled to electron transfer processes. The oxidized and reduced forms of the protein, each with a different equilibrium conformation, have different electron transfer kinetics and formal potentails. We assumed that the conformational changes were fast on the voltammetric time scale of seconds, and used digital simulations based on Scheme 3 featuring an oxidized form of the enzyme reduced at a moderate rate, and a reduced form oxidized at a faster rate. This *E reduction/E oxidation* model provided best fits to the experimental data (Figure 5) using rate constants $k_{s,ox} \geq 10\ k_{s,red}$, where $k_{s,red}$ was fixed at the k_s value found from the Laviron analysis. These simulations are fully consistent with Scheme 3 involving fast conformational equilibria between oxidized and reduced forms of cyt P450s in the films.[48] Important features of the

modified square scheme model (Scheme 3) involve the different formal potentials and electron transfer rates for oxidation and reduction. This model fits the cyt P450 voltammetry data well, but more subtle factors may also be operating that are not readily apparent from the voltammetry.[48]

The heterogeneous electron transfer rate constants $k_{s,red}$ for reduction of the cyt P450s depended strongly on heme iron spin state. That is, low spin cyt$P450_{cam}$ had a 40-fold larger $k_{s,red}$ than high spin human cyt P450 1A2, and mixed spin human P450 cyt 2E1 had an intermediate value. This result is consistent with biochemical studies showing faster reduction of low spin cyt P450s 1A2 and 2E1 compared to high spin forms.[70-72]

IV. Kinetics of ferryloxy cyt P450 formation

As discussed above, the proposed active ferryloxy radical cation $^{\bullet+}$(P450-Fe^{IV}=O) can be produced by oxidation with peroxide. In electrochemical reduction of iron heme proteins P450-Fe^{III} in aerobic solution, reduced PFe^{II} combines with dioxygen to form PFe^{II}-O_2 complexes. This complex is reduced electrochemically yielding hydrogen peroxide and regenerating the PFe^{II}-heme.[25,26,39,] The peroxide generated in this catalytic reduction of oxygen reacts with cyt P450Fe^{III} to form $^{\bullet+}$(P450-Fe^{IV}=O), which gets reduced at the electrode to regenerate cyt P450-Fe^{III} (Scheme 4A). This produces a catalytic current that can be analyzed to evaluate the kinetics of formation of the active oxidant. A straightforward way to oxidize cyt P450Fe^{III} into $^{\bullet+}$(P450-Fe^{IV}=O) is to add organic peroxide like t-BuOOH (Scheme 4B) and observe the catalytic current by rotating disc voltammetry.[48]

In rotating disc voltammetry (RDV) of catalytic films, limiting current for a reaction at steady-state is related to interfacial electron exchange, enzyme kinetics, and substrate mass transport by [37d,73]

$$\frac{1}{I_L}=\frac{1}{I_{Lev}}+\frac{1}{I_E}+\frac{1}{I_{cat}} \quad (1)$$

where I_L is limiting current; I_E is exchange current due to interfacial electron transfer between the electrode and enzyme; I_{cat} is the catalytic current resulting from substrate conversion by the enzyme, and I_{Lev} is the Levich current related to transport of substrate from the bulk solution to the film. At high overpotential, I_E can be neglected. I_{cat} is obtained by extrapolating I_L to infinite rotation rate at each substrate concentration. To conserve valuable enzyme, relative kinetic parameters can be estimated at a large rotation rate by taking I_L to approximate relative I_{cat} values.[48,73]

The catalytic current (I_{cat}) is given by an electrochemical version of the Michaelis-Menten enzyme kinetics equation,[37a]

$$I_{cat}=\frac{nFA\Gamma(k_{cat}/K_M)C_s}{(1/K_M)C_s+1} \quad (2)$$

where n is the number of electrons in the electrochemical reaction (n = 2, Scheme 3B); F is Faraday's constant; A is electrode area, Γ is electroactive surface concentration of enzyme in the film, C_s is substrate concentration in solution, k_{cat} is the catalytic rate constant (s^{-1}) assumed to be rate limiting, and K_M is Michaelis-Menten dissociation constant.

Rotating disk voltammetry of cyt P450/polyion LbL films[48] showed increases in catalytic limiting reduction current with increasing concentration of t-BuOOH (Figure 6 A,B).

Limiting current densities were taken as approximations to I_{cat}/A and converted to relative enzyme turnover as $I_{cat}/A/\Gamma$. These values vs. C_s were fit onto eq 2 to obtain apparent K_M and k_{cat} (Figure 6C). The ratio of k_{cat} to K_M provides a measure of relative catalytic efficiency with units of a second order rate constant. Relative k_{cat}/K_M values for oxidation of ferric cyt P450s in films to ferryloxy forms by t-butyl hydroperoxide suggested a dependence on spin state in the reverse order of that observed for the electrochemical hET reduction rate constants. That is, high spin cyt P450s were oxidized faster than low spin. Oxidation and reduction kinetics of cyt P450s in the films also depend on protein secondary structure near the active site.[48]

V. Mimicking *in vivo* cyt P450 pathways

None of the cyt P450 biocatalytic systems described above accurately mimic all the features of the natural catalytic cycle (Scheme 1), namely electron injection into molecular CPR, then complexation and electron transfer to the enzyme. However, we showed in 2005 by direct voltammetry in thin films of genetically engineered microsomes containing cyt P450s 1A2 and 3A4 that electrons enter the films via CPR.[74] Cyt P450s in these films oxidized styrene with low catalytic activity. Reasonably good catalytic turnover of microsomal cyt P450 3A4/CPR for testosterone conversion in films on special hydrophobic electrodes was achieved by Mie et al.[75] Enhanced catalytic efficiency was attributed to electron transfer from electrode to CPR to cyt P450 3A4. A mixed catalytic pathway is probably operative in this system as the authors also claimed direct electron transfer to cyt P450 3A4.

We fabricated films using CPR microsomes, but added pure cyt P450s to achieve a large ratio of cyt P450 to CPR (Scheme 5) as in the human liver.[1,2] These 30 nm thick films efficiently mimic the natural cyt P450 biocatalytic pathway,[76] with initial electron injection from electrode to CPR, then to cyt P450. Cyt $P450Fe^{II}$-CO spectral bands at 450 nm were found for all films, confirming presence of the native enzyme (Figure 3 C, D). Films of microsomal CPR/cyt P450 had formal potentials near -250 mV vs NHE (Figure 7A), no CV potential shifts when CO was added, and k_s values near 40 s^{-1}, similar to films with only CPR or CPR and cyt b_5 (present in some microsomal preparations). In contrast, films containing cyt P450s (Figure 7B) but no CPR had redox potentials near -100 mV vs NHE, gave ~40 mV shifts with CO, and had >50% smaller k_s values. These data unequivocally support injection of electrons into CPR and not cyt P450.

An interesting and unusual feature of these voltammograms compared to films of only CPR was that cyt P450s caused large increases in both reduction and oxidation peak currents. This is a consequence of the pathway in Scheme 6, in which CPR is reduced (eq 3), and the reduced form of CPR_{red} is involved in a chemical redox equilibrium with cyt $P450Fe^{III}$ to produce CPR_{ox} (eq 4), as well as an electrochemical oxidation (eq 5). This pathway was used to accurately simulate voltammograms and trumpet plots for the CPR/cyt P450 films using the best fit parameters shown in Scheme 6.[76] As with cyt P450 films, individual values of $k_{s,red}$ and $k_{s,ox}$ were required to achieve accurate fits to the experimental data.

Electron transfer from electrode to CPR to cyt P450 was further confirmed by observing catalytic limiting current by RDV for oxidation of 4-(methylnitrosamino)-1-(3-pyridyl)-1-butanone (NNK) (Figure 8). NNK conversion by human cyt P450s 1A2 and 2E1 yields 4-hydroxy-1-(3-pyridyl)-1-butanone (HPB), [77] and HPB was identified by LC-MS as the electrolysis product.[76] Biocatalytic electrode-driven NNK oxidation was ~1.5 times more efficient than the NADPH-driven reaction in the same films. While electron flow is not likely to be equivalent in these experiments, electrochemical biocatalysis was at least as efficient as the NADPH-driven process.

The E_rCE_o model used for simulations of CVs is thus further supported by the electrode-driven catalytic turnover described above. These simulations also provided a means to probe the key equilibrium electron exchange between cyt P450 and CPR (eq 4). The best fit condition $k_b \geq 5k_f$ indicates that in the absence of O_2 the equilibrium with $K = k_f/k_b \leq 0.2$ lies to the left, in favor of CPR_{red}. This suggests why CPR_{ox} is reduced electrochemically in cyt P450/CPR films instead of cyt P450, even though without CPR, cyt P450s have a 150 mV more positive reduction potential. The redox potential difference ($\Delta E°$) between CPR and cyt P450 is given by $\Delta E° = [RT/nF] \ln(K)$. Having $K<0.2$ dictates that the cyt P450 redox potential is shifted more negative than that of CPR_{ox} by 40 mV or more. Thus, CPR_{ox} is more easily reduced than the cyt P450s consistent with a 140 mV shift in redox potential of cyt P450s in the cyt P450/CPR films compared to cyt P450 in films without CPR. The most likely cause of this large potential shift is complexation of cyt P450s with CPR, which has been proposed as a key feature of cyt P450 catalytic cycles for decades.[1,2]

Further, $K \leq 0.2$ suggests that most CPR during film voltammetry is stored as CPR_{red}. When oxygen and substrate are added, equilibrium in eq 4 is driven to the right by rapid removal of cyt P450-Fe^{II} by the catalytic steps (Scheme 1). This causes more CPR_{red} to be formed by electrochemical reduction to efficiently drive the catalysis. We can only speculate that a similar process in the natural catalytic cycle, with storage of reducing power in CPR_{red}, might be a factor in how CPR addresses such a large excess of cyt P450s.

VI. Summary and Future Perspectives

In this article, we described three different ways to effectively utilize electrode-driven cyt P450 biocatalysis using thin films. First, direct electron transfer in aerobic solutions results in catalytic reduction of oxygen producing hydrogen peroxide that activates cyt P450Fe^{III} in films to the active ferryloxy radical cation. A variation of this approach is to add peroxide, an approach that can be used to measure ferryloxy formation kinetics using voltammetry. Work in this area has produced some systems with good catalytic activity, and others that do not seem very active. Relevant to this approach, our recent voltammetric investigations of several human and bacterial cyt P450s showed that the kinetics of voltammetric reduction and peroxide mediated cyt P450 oxidation depend in opposite ways on the spin state of the iron heme, and also on the secondary polypeptide structure in the vicinity of the active site.[48]

A second way of electrochemically activating cyt P450s is by the use of fusion proteins, in which an initial electron acceptor protein is linked to a cyt P450. Electrons flow from the electrode, to the initial electron acceptor, to the cyt P450. Recent studies suggest that biocatalysis using cyt P450 fusion proteins can be optimized by controlling the initial electron transfer rate.[22]

Third, microsomal CPR/cyt P450 films on electrodes most closely mimic the natural catalytic pathway. Electrons flow from the electrode to CPR to the cyt P450 as in the in vivo pathway. In addition to biocatalysis, these films can be used to obtain mechanistic insights using voltammetry and digital simulations.[76] As this method is closest to the natural pathway, we expect it has the best chance to retain all the important features of cyt P450-based metabolism such as high regiospecificity and stereoselectivity. However, based on results published so far, it is likely that all of the methods of electrochemical biocatalysis are capable of characteristic cyt P450 substrate conversion.

Given the above three alternatives, applications requiring efficient catalytic turnover of substrates by cyt 450s would seem to have a bright future. These enzyme systems with valuable synthetic capabilities can achieve carbon hydroxylation, epoxidation, dealkylation, heteroatom oxygenation, ester cleavage, cyclization, and isomerization,[78] and have the

potential for an excellent future for NADPH-free chemical synthesis, drug development and toxicity screening.[79] Also, recent reviews have emphasized protein engineering to optimize catalytic properties of cyt P450s for synthetic applications.[22,80] While obtaining sufficient materials for these application can be time consuming, one approach is to use genetically engineered bacteria to isolate bicistronic membrane-bound materials featuring lipid, a single cyt P450, and CPR. These systems can be used directly to fabricate LbL films.[81] They have high catalytic activity, the ability to accurately mimic the natural pathway, and are isolated and purified in less than 10% of the time required for isolation and purification of pure cyt P450s.[79]

We envision future practical implementation of electrochemical arrays of natural and engineered cyt P450s for drug toxicity screening and synthetic applications that are simpler than NADPH-driven arrays that we have previously developed.[79,81] Also, microsomal CPR/cyt P450 films in particular provide the opportunity for detailed insights into how features such as iron heme spin state, and polypeptide secondary structure near the distal and proximal sites of the heme cyt P450s impact electron transfer kinetics, reaction pathways, and biocatalytic properties. This knowledge should allow tailoring the best cyt P450 isoforms, engineered structures, and film configurations to achieve specific organic transformations with high efficiency.

Acknowledgments

This work was financially supported by U.S. PHS grant ES03154 from the National Institute of Environmental Health Sciences (NIEHS), NIH.

References

1. Schenkman, JB.; Greim, H., editors. Cytochrome P450. Springer-Verlag; Berlin: 1993.
2. Ortiz de Montellano, PR., editor. Cytochrome P450. Kluwer/Plenum; New York: 2005.
3. Kramer JA, Sagartz JE, Morris DL. Nature Rev. Drug Discov. 2007; 6:636–649. [PubMed: 17643090]
4. Sansen S, Yano JK, Reynald RL, Schoch GA, Griffin KJ, Stout CD, Johnson EF. J. Biol. Chem. 2007; 282:14348–14355. [PubMed: 17311915]
5. Porubsky PR, Meneely KM, Scott EE. J. Biol. Chem. 2008; 283:33698–33707. [PubMed: 18818195]
6. Poulos TL, Finzel BC, Howard AJ. J. Mol. Biol. 1987; 195:687–700. [PubMed: 3656428]
7. Moreland JL, Gramada A, Buzko OV, Zhang Q, Bourne PE. BMC Bioinformatics. 2005; 6:21. [PubMed: 15694009]
8. Schenkman JB, Jansson I. Pharmacology & Therapeutics. 2003; 97:139–152. [PubMed: 12559387]
9. Shimada T, Mernaugh RL, Guengerich FP. Arch. Biochem. Biophys. 2005; 435:207–216. [PubMed: 15680923]
10. Nordblom GD, White RE, Coon MJ. Arch. Biochem. Biophys. 1976; 175:524–533. [PubMed: 8710]
11. Guengerich FP. Chem. Res. Toxicol. 2001; 14:611–650. [PubMed: 11409933]
12. Meunier B, de Visser SP, Shaik S. Chem. Rev. 2004; 104:3947–3980. [PubMed: 15352783]
13. Guengerich FP. J. Biochem. Mol. Toxicol. 2007; 21:163–168. [PubMed: 17936929]
14. Ioannidis C, Lewis DFV. Curr.Topics Med.Chem. 2004; 4:1767–1788.
15. Vilker, VL.; Khan, F.; Shen, D.; Baizer, MM.; Nobe, K. Redox chemistry and interfacial behavior of biological molecules. Dryhurst, G.; Niki, K., editors. Plenum Press; New York: 1988. p. 105-112.
16. Kazlauskaite J, Westlake ACG, Wong L-L, Hill HAO. Chem. Commun. 1996:2189–2190.
17. Rusling JF, Hvastkovs EG, Hull DO, Schenkman JB. Chem. Commun. 2008:141–154.

18. Zhang Z, Nassar A-EF, Lu Z, Schenkman JB, Rusling JF. J. Chem. Soc. Faraday Trans. 1997; 93:1769–1774.
19. Lvov YM, Lu Z, Schenkman JB, Zu X, Rusling JF. J. Am. Chem. Soc. 1998; 120:4073–4080.
20. Bistolas N, Wollenberger U, Jung C, Scheller FW. Biosens. Bioelec. 2005; 20:2408–2423.
21. Fleming BD, Johnson DL, Bond AM, Martin LL. Expert Opin. Drug Metab. Toxicol. 2006; 2:581–589. [PubMed: 16859406]
22. Dodhia, VR.; Gilardi, G. Engineering the Bioelectronic Interface: Applications to Analyte Biosensing and Protein Detection. Davis, J., editor. RSC publications; 2009. p. 153-189.
23. Zu X, Lu Z, Zhang Z, Schenkman JB, Rusling JF. Langmuir. 1999; 15:7372–7377.
24. Munge B, Estavillo C, Schenkman JB, Rusling JF. ChemBiochem. 2003; 4:82–89. [PubMed: 12512080]
25. Rusling, JF.; Zhang, Z. Biomolecular Films. Rusling, JF., editor. Marcel Dekker; New York: 2003. p. 1-64.
26. Rusling, JF.; Wang, B.; Yun, SE. Bioelectrochemistry. Bartlett, PN., editor. John Wiley; New York: 2008. p. 39-86.
27. Nobe, K.; Baizer, MM.; Shen, DH.; Vilker, VL.; Cho, AK. Electro organic synthesis: festschrift for Manuel M. Baizer. Little, RD.; Weinberg, NL., editors. Marcel Dekker Inc.; New York: 1991. p. 265-271.
28. Reipa V, Mayhew MP, Vilker VL. Proc. Natl. Acad. Sci. USA. 1997; 94:13554–13558. [PubMed: 9391064]
29. Mak LH, Sadeghi SJ, Fantuzzi A, Gilardi G. Anal. Chem. 2010; 82:5357–5362. [PubMed: 20507171]
30. Yeh P, Kuwana T. Chem. Lett. 1977:1145–1148.
31. Eddowes MJ, Hill HAO. Chem. Commun. 1977:3154–3155.
32. Armstrong FA, Hill HAO, Walton NJ. Acc. Chem. Res. 1988; 21:407–413.
33. Scheller F, Renneberg R, Strnad G, Pommerening K, Mohr P. Bioelectrochem. Bioenerg. 1977; 4:500–507.
34. a Faulkner KM, Shet MS, Fisher CW, Estabrook RW. Proc. Natl. Acad. Sci. USA. 1995; 92:7705–7709. [PubMed: 7644480] b Estabrook RW, Faulkner KM, Shet MS, Fisher CW. Methods Enzymol. 1996; 272:44–50. [PubMed: 8791761]
35. Udit AK, Arnold FH, Gray HB. J. Inorg. Biochem. 2004; 98:1547–1550. [PubMed: 15337607]
36. Zilly FE, Taglieber A, Schulz F, Hollmann F, Reetz MT. Chem. Commun. 2009:7152–7154.
37. a Sucheta A, Cammack R, Weiner J, Armstrong FA. Biochemistry. 1993; 32:5455–5465. [PubMed: 8499449] b Armstrong FA, Heering HA, Hirst J. J. Chem. Soc. Rev. 1997; 26:169–179.c Armstrong FA, Wilson GS. Electrochim. Acta. 2000; 45:2623–2645.d Heering HA, Hirst J, Armstrong FA. J. Phys. Chem. B. 1998; 102:6889–6902.e Leger C, Elliott SJ, Hoke KR, Jeuken LJC, Jones AK, Armstrong FA. Biochemistry. 2003; 42:8653–8662. [PubMed: 12873124] f Vincent KA, Parkin A, Armstrong FA. Chem. Rev. 2007; 107:4366–4413. [PubMed: 17845060]
38. Armstrong, FA. Bioelectrochemistry of Biomacromolecules: Bioelectrochemistry: Principles and Practice. Lenaz, G.; Milazo, G., editors. Birkhauser Verlag; Basel: 1997. p. 205-255.
39. Rusling, JF.; Zhang, Z. Handbook of surfaces and interfaces of materials: Biomolecules, Biointerfaces, and Applications. Nalwa, RW., editor. Vol. 5. Academic Press; 2001. p. 33-71.
40. Davis JJ, Hill HAO. Chem. Comm. 2002:393–401. [PubMed: 12120511]
41. a Yang M, Kabulski JL, Wollenberg L, Chen X, Subramanian M, Tracy TS, Lederman D, Gannett PM, Wu N. Drug Metab. Dispos. 2009; 37:892–899. [PubMed: 19171677] b Todorovic S, Jung C, Hildebrandt P, Murgida DH. J. Biol. Inorg. Chem. 2006; 11:119–127. [PubMed: 16328458]
42. Ferrero VEV, Andolfi L, Nardo GD, Sadeghi SJ, Fantuzzi A, Cannistraro S, Gilardi G. Anal. Chem. 2008; 80:8438–8446. [PubMed: 18947200]
43. Fantuzzi A, Fairhead M, Gilardi G. J. Am. Chem. Soc. 2004; 126:5040–5041. [PubMed: 15099066]
44. Tanvir S, Pantigny J, Boulnois P, Pulvin S. J. Membr. Sci. 2009; 329:85–90.

45. Mak LH, Sadeghi SJ, Fantuzzi A, Gilardi G. Anal. Chem. 2010; 82:5357–5362. [PubMed: 20507171]
46. Udit AK, Gray HB. Biochem. Biophys. Res. Commun. 2005; 338:470–476. [PubMed: 16139241]
47. Dodhia VR, Sassone C, Fantuzzi A, Nardo GD, Sadeghi SJ, Gilardi G. Electrochem. Commun. 2008; 10:1744–1747.
48. Krishnan S, Abeykoon A, Schenkman JB, Rusling JF. J. Am. Chem. Soc. 2009; 131:16215–16224. [PubMed: 19886700]
49. Lvov, Y. Handbook of Surfaces and Interfaces of Materials. Nalwa, RW., editor. Vol. 3. Academic Press; San Diego: 2001. p. 170-189.
50. Kamau GN, Guto MP, Munge B, Panchagnula V, Rusling JF. Langmuir. 2003; 19:6976–6981.
51. Bismuto E, Sirangelo I, Irace G. Arch. Biochem. Biophys. 1992; 298:624–629. [PubMed: 1416991]
52. Panchagnula V, Kumar CV, Rusling JF. J. Am. Chem. Soc. 2002; 124:12515–12521. [PubMed: 12381195]
53. Hvastkovs EG, So M, Krishnan S, Bajrami B, Tarun M, Jansson I, Schenkman JB, Rusling JF. Anal. Chem. 2007; 79:1897–1906. [PubMed: 17261025]
54. Guto PM, Rusling JF. Electrochem. Commun. 2006; 8:455–459.
55. Evans DF, Ninham BW. J. Phys. Chem. 1986; 90:226–234.
56. Lee C-Y, Bond AM. Langmuir. 2010; 26:5243–5253. [PubMed: 20232815]
57. Gao Z, Frank HA, Lvov YM, Rusling JF. Bioelectrochemistry. 2001; 54:97–100. [PubMed: 11506980]
58. Udit AK, Hagen KD, Goldman PJ, Star A, Gillan JM, Gray HB, Hill MG. J. Am. Chem. Soc. 2006; 128:10320–10325. [PubMed: 16881664]
59. Wiwatchaiwong S, Matsumura H, Nakamura N, Yohda M, Ohno H. Electroanalysis. 2007; 19:561–565.
60. Koo LS, Immoos CE, Cohen MS, Farmer PJ, Ortiz de Montellano PR. J. Am. Chem. Soc. 2002; 124:5684. [PubMed: 12010041]
61. Immoos CE, Chou J, Bayachou M, Blair E, Greaves J, Farmer PJ. J. Am. Chem. Soc. 2004; 126:4934–4942. [PubMed: 15080699]
62. Blair E, Greaves J, Farmer PJ. J. Am. Chem. Soc. 2004; 126:8632–8633. [PubMed: 15250698]
63. Rudakov YO, Shumyantseva VV, Bulko TV, Suprun EV, Kuznetsova GP, Samenkova NF, Archakov AI. J. Inorg. Biochem. 2008; 102:2020–2025. [PubMed: 18842301]
64. Estavillo C, Lu Z, Jansson I, Schenkman JB, Rusling JF. Biophys. Chem. 2003; 104:291–296. [PubMed: 12834847]
65. Laviron E. J. Electroanal. Chem. 1979; 101:19–28.
66. Feldberg SW, Rubinstein I. J. Electroanal. Chem. 1988; 240:1–15.
67. Kasmi AE, Leopold MC, Galligan R, Robertson RT, Saavedra SS, Kacemi KE, Bowden EF. Electrochem. Commun. 2002; 4:177–181.
68. Hoffman BM, Ratner MA. J. Am. Chem. Soc. 1987; 109:6237–6243. references therein.
69. Hirst J, Armstrong FA. Anal. Chem. 1998; 70:5062–5071. [PubMed: 9852788]
70. Yamazaki H, Ueng Y-F, Shimada T, Guengerich FP. Biochem. 1995; 34:8380–8389. [PubMed: 7599128]
71. Yamazaki H, Johnson WW, Ueng Y-F, Shimada T, Guengerich FP. J. Biol. Chem. 1996; 271:27438–27444. [PubMed: 8910324]
72. Guengerich FP, Johnson WW. Biochem. 1997; 36:14741–14750. [PubMed: 9398194]
73. Guto PM, Rusling JF. J. Phys. Chem. B. 2005; 109:24457–24464. [PubMed: 16375448]
74. Sultana N, Schenkman JB, Rusling JF. J. Am. Chem. Soc. 2005; 127:13460–13461. [PubMed: 16190685]
75. Mie Y, Suzuki M, Komatsu Y. J. Am. Chem. Soc. 2009; 131:6646–6647. [PubMed: 19402636]
76. Krishnan S, Wasalathanthri D, Zhao L, Schenkman JB, Rusling JF. J. Am. Chem. Soc. 2011; 133:1459–1465. [PubMed: 21214177]
77. Hecht SS. Chem. Res. Toxicol. 1998; 11:559–603. [PubMed: 9625726]

78. Coon MJ. Annu. Rev. Pharmacol. Toxicol. 2005; 45:1–25. [PubMed: 15832443]

79. Rusling, JF.; Hvastkovs, EG.; Schenkman, JB. Drug Metabolism Handbook. Nassar, A.; Hollenburg, PF.; Scatina, J., editors. Wiley; New Jersey: 2009. p. 307-340.

80. Gillam EMJ. Chem. Res. Toxicol. 2008; 21:220–231. [PubMed: 18067267]

81. Krishnan S, Bajrami B, Hvastkovs EG, Choudhary D, Schenkman JB, Rusling JF. Anal Chem. 2008; 80:5279–5285. [PubMed: 18563913]

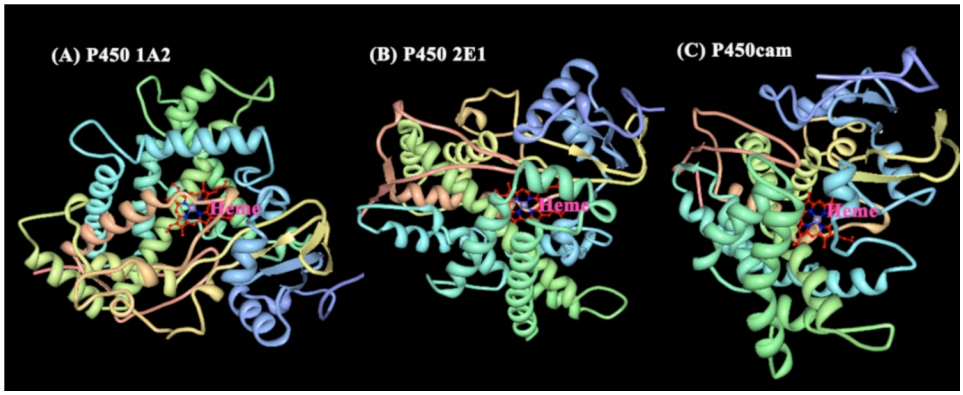

Figure 1.
X-ray crystal structures of human cyt P450s (A) 1A2 (PDB:2HI4);[4] (B) 2E1 (PDB:3E4E);[5] and (C) bacterial cyt $P450_{cam}$ (PDB:2CPP).[6] Structures were obtained from the protein data bank.[7]

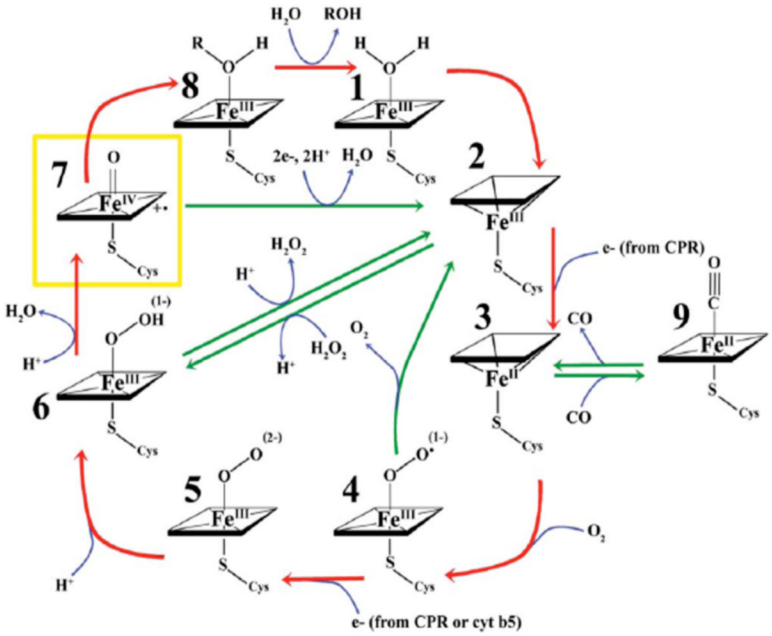

Scheme 1.
Proposed cyt P450 catalytic cycle.[2, 11,17]

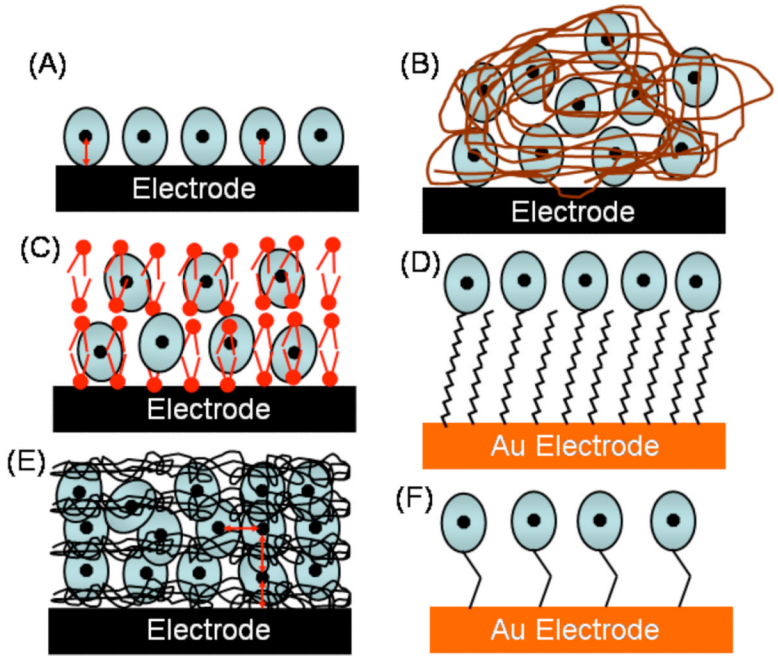

Scheme 2.

Immobilization strategies for protein film voltammetry and biocatalysis: (A) adsorbed protein film; (B) cast films of protein and polyions; (C) cast films of proteins and insoluble lipids; (D) proteins on self-assembled alkylthiol monolayers on Au; (E) LbL films of enzyme and polyions; (F) covalently immobilized proteins.

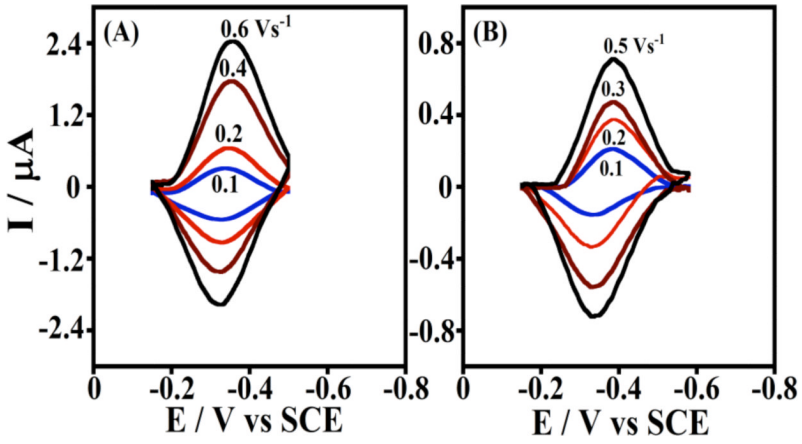

Figure 2.

Background subtracted cyclic voltammograms of LbL films on PG electrodes in anaerobic 50 mM potassium phosphate buffer + 0.1 M NaCl, pH 7.0:[48] (A) cyt P450 2E1/polyion and (B) cyt $P450_{cam}$/polyion. Reproduced with permission from ref. 48, American Chemical Society, copyright 2009.

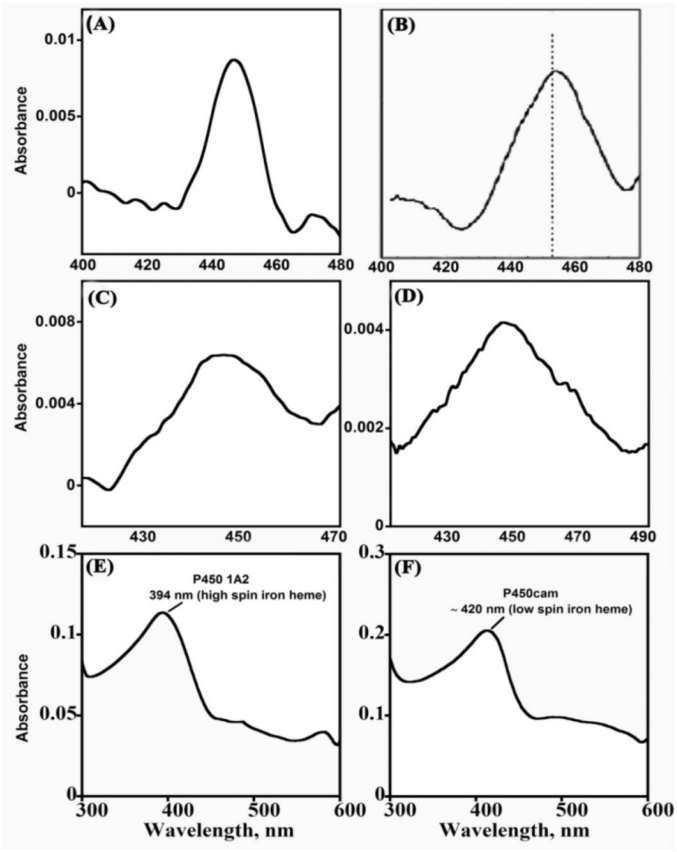

Figure 3.

Spectra of cyt P450 films on aminosilane-functionalized silica slides in pH 7.0 buffer. **(A to D)** Difference spectra after reducing enzyme to ferrous form and adding CO: (A) polyion/cyt P450 1A2; (B) polyion/cyt $P450_{cam}$; (C) Cyt P450 1A2/CPR films reduced directly with sodium dithionite or (D) reduced via CPR using 1 mM NADPH. (**E and F**) Ferric enzyme film spectra: (E) Ferric polyion/cyt P450 1A2 showing high spin heme iron and (F) ferric polyion/cyt $P450_{cam}$ showing low spin heme iron of $P450_{cam}$ in LbL films. Reproduced with permission (A), (E) and (F) from ref. 48; (B) from ref. 53, American Chemical Society, copyright 2009 & 2007; (C) & (D) from ref. 76, American Chemical Society, copyright 2011.

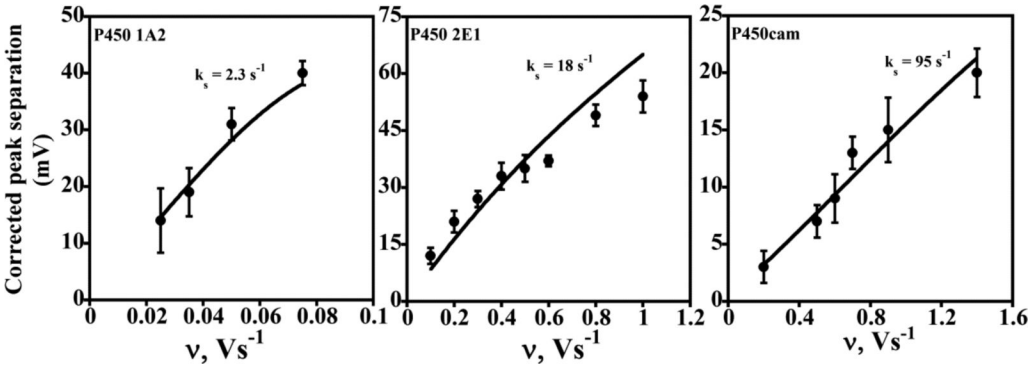

Figure 4.

Influence of cyclic voltammetry scan rate for different cyt P450/polyion LbL films (as denoted on each plot) on experimental (•) peak separation (ΔE_p) corrected for scan rate independent non-kinetic contribution. The theoretical lines were computed for Butler-Volmer theory for the rate constant (k_s) values shown for transfer coefficient α= 0.5. Reproduced with permission from ref. 48, American Chemical Society, copyright 2009.

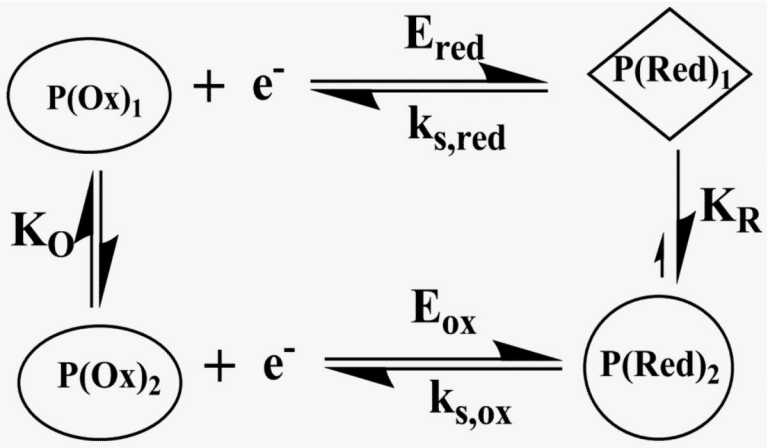

Scheme 3.
Modified square scheme for thin film voltammetry of cyt P450s.

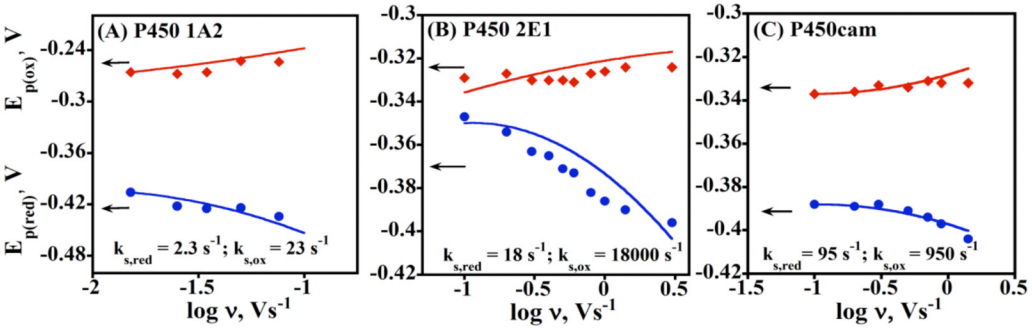

Figure 5.

Oxidation and reduction peak potentials vs. log scan rate for cyt P450 films from CVs of LbL films of (A) Polyion/P450 1A2; (B) Polyion/P450 2E1; and (C) Polyion/$P450_{cam}$. Experimental oxidation (red diamonds) and reduction (blue circles) peak potentials are shown along with the best fit simulations (lines) obtained by using an *E reduction/E oxidation* mechanism with the reduction ($k_{s,red}$) and oxidation ($k_{s,ox}$) rate constants shown in each plot.[48] Reproduced with permission from ref. 48, American Chemical Society, copyright 2009.

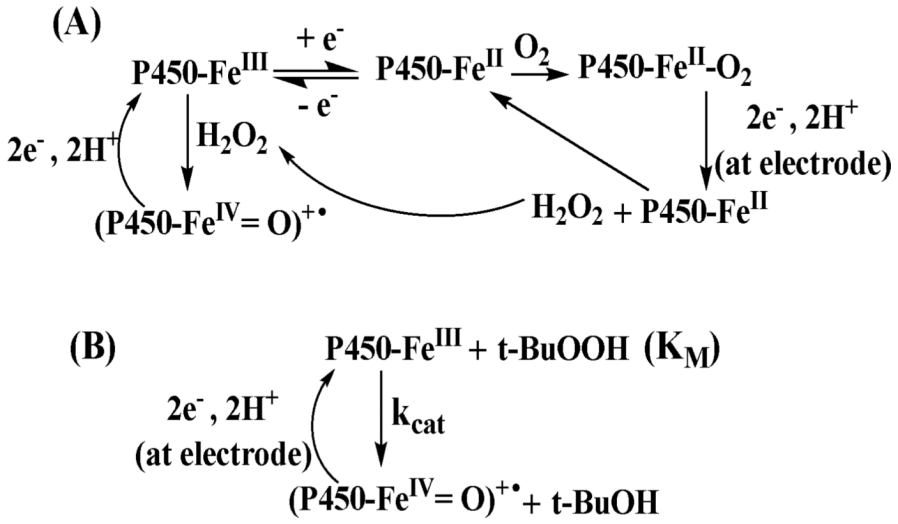

Scheme 4.

Pathways for biocatalytic activation of cyt P450s by peroxides: (A) oxygen reduction formed peroxide by cyt P450s on electrodes; (B) t-butyl hydroperoxide (t-BuOOH) reduction by cyt P450s.

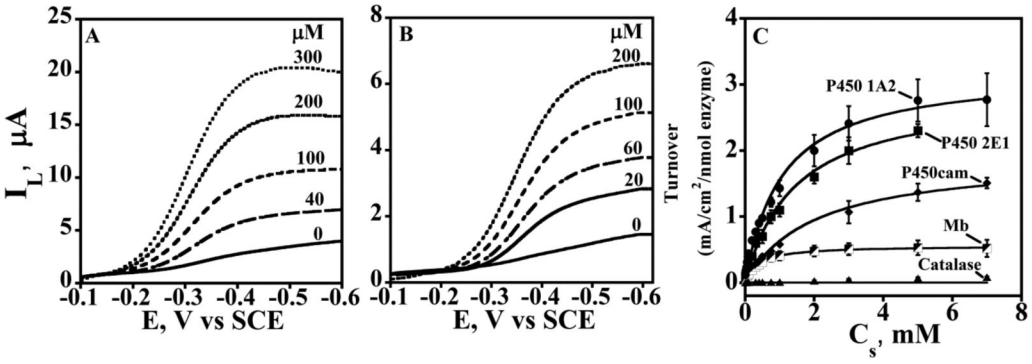

Figure 6.

Rotating disk voltammograms of cyt P450 films on PG electrodes for t-BuOOH reduction in anaerobic potassium phosphate buffer (pH 7.0) at 25 °C. Limiting currents (I_L) for increasing t-BuOOH concentration (in μM) are shown for (A) polyion/P450 2E1 and (B) polyion/P450cam LbL films. (C) Plots of apparent enzyme turnover rate (I_L/Γ) vs. t-BuOOH concentration for cyt P450 films shown along with control myoglobin (Mb) and catalase films. Symbols are experimental data and solid lines represent Michaelis-Menten fit (eq. 2) from which kinetic parameters k_{cat} and K_M were obtained. Reproduced from ref. 48 with permission from American Chemical Society, copyright 2009.

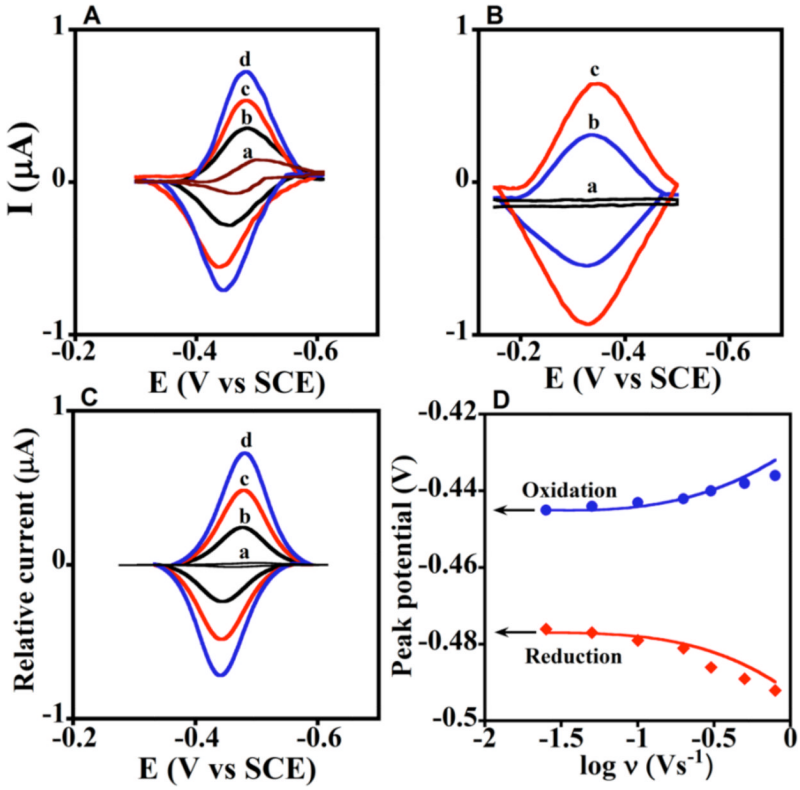

Figure 7. Experimental and simulated voltammetry for films of cyt P450 1A2 and CPR microsomes

(**A)** Background subtracted CVs of **a,** CPR films at 0.3 V s^{-1} with no cyt P450, and **b-d,** cyt P450 1A2 + CPR films at scan rates (b) 0.1, (c) 0.2, and (d) 0.3 Vs^{-1}. (**B)** background subtracted CVs: **a,** polyion film, and **b-c,** cyt P450 1A2 film with no CPR at (b) 0.1 and (c) 0.2 V s^{-1}. (**C**) Digitally simulated theoretical CVs corresponding to **a,** reversible electron transfer for only CPR film at 0.3 Vs^{-1}, and **b-d,** the E_rCE_o-model and parameters in Scheme 6 for cyt P450 1A2 + CPR films at scan rates (b) 0.1, (c) 0.2, and (d) 0.3 V s^{-1} showing excellent agreement with the experimental CVs in Figure 7A. (**D)** Influence of scan rate on oxidation (blue circles) and reduction (red diamonds) peak potentials for cyt P450 1A2 + CPR films plotted with theoretical peak potentials (lines) simulated using the E_rCE_o model. Reproduced with permission from ref. 76, American Chemical Society, copyright 2011.

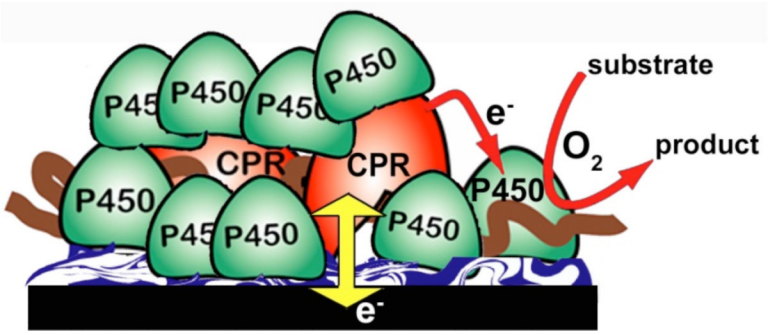

Scheme 5.
Microsomal CPR/Cyt P450 films that mimic the natural catalytic pathway on an electrode.

$$CPR_{ox} + e \rightarrow CPR_{red} \qquad E^{o\prime} = -230 \text{ mV vs. NHE; } k_{s,red} = 0.4 \text{ s}^{-1} \qquad (3)$$

$$CPR_{red} + P450\text{-}Fe^{III} \rightleftharpoons CPR_{ox} + P450\text{-}Fe^{II} \qquad k_b \geq 5k_f \qquad (4)$$

$$CPR_{red} - e \rightarrow CPR_{ox} \qquad E^{o\prime} = -230 \text{ mV vs. NHE; } k_{s,ox} = 40 \text{ s}^{-1} \qquad (5)$$

Scheme 6.

E_rCE_o simulation model for CVs of cyt P450s + CPR.[76]

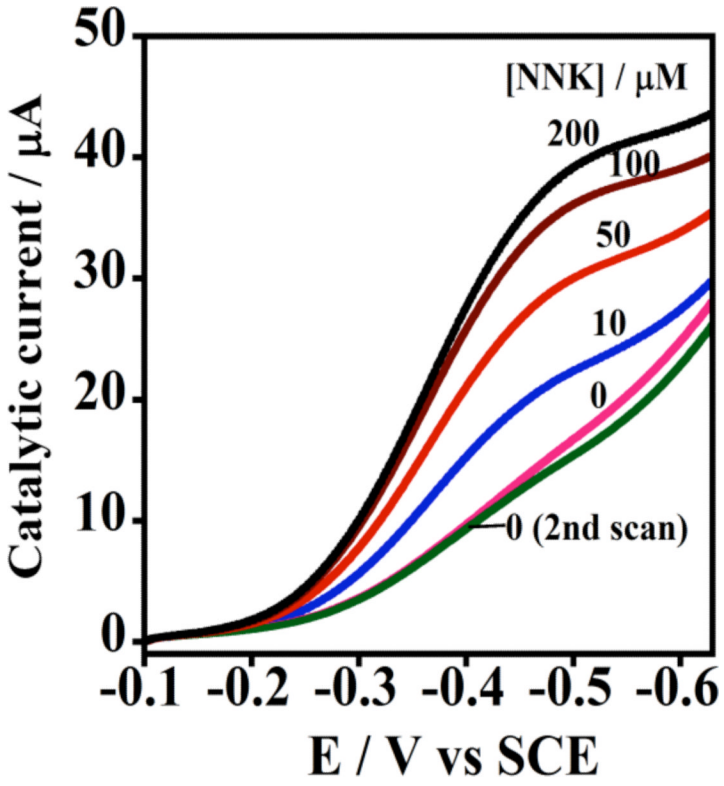

Figure 8. Catalytic rotating disk voltammetry of Cyt P450 + CPR films

Increase in steady state current with increasing concentration of substrate 4-(methylnitrosamino)-1-(3-pyridyl)-1-butanone (NNK) in pH 7.0 buffer. Reproduced with permission from ref. 76, American Chemical Society, copyright 2011.